A Novel Microactuator Device Based on Magnetic Nanofluid.

Alexandru M. Morega[*,**], *Senior Member, IEEE*
[*] University POLITEHNICA of Bucharest, Faculty of Electrical Engineering, UPB-EE, Bucharest, ROMANIA
[**] "Gheorghe Mihoc – Caius Iacob" Institute of Applied Mathematics, Romanian Academy
Email: amm@iem.pub.ro
Lucian Pîslaru-Dănescu[**]
[***]Microelectromechanical Department, National Institute for Electrical Engineering, ICPE-CA, Bucharest, ROMANIA
Email: paslaru@icpe-ca.ro
Mihaela Morega[*], *Member, IEEE*
Email: mihaela@iem.pub.ro

***Abstract*—This paper presents the prototype of an actuator that utilizes a colloidal, super-paramagnetic, nanometric particles fluid as active medium. The experimental measurements show that magnetic properties of the fluid are adequate to the actuator working conditions.**

An electronic module for the control of the actuator ferrite cored coils was designed and produced; it implements the pulse width modulation (PWM) principle. The module produces train pulses of adjustable frequency and fill factor to drive the electrical currents in the actuator coils.

The magnetic field produced by the actuator coils generates magnetic body forces in the magnetic fluid that add to gravitational forces to drive the fluid in a forced flow. The motion is perceived as periodic stationary surface waves, localized above the actuator coils. Mathematical modeling and numerical simulation (by the finite element method (FEM)) are used to study and evaluate these processes. The heat transfer part of the problem was also studied, although thermal stability proves to be less of a concern.

The device may provide a usable actuation resolution, as the results suggests.

I. INTRODUCTION

Ferrofluid technology is able to solve various technical problems, such as noise reduction, accurate positioning, sealing, and it becomes widely used as a new concept for the design of several devices: actuators, "silent" coils, sensors, (*e.g.*, accelerometers, flowmeters, sensors for inclination, pressure, level, *etc*.), sealing systems, different types of contacts [1], *etc*. Because the occurring magnetization body forces may be controlled by adjusting the incident magnetic fields ferrofluids can be precisely positioned and controlled [2–7].

Ferrofluids are increasingly used for actuator damping in a variety of devices including speakers [8], CD and Laser Disc players, CD-ROM and DVD-ROM drives [1]. Finally, another noteworthy application is represented by deformable mirrors made out of a magnetic liquid, whose surface is actuated by a hexagonal array of small current carrying coils [9].

Magnetizable fluids with a lower concentration of magnetic nanoparticles, which emerge with the advent of nanotechnology, exhibit superior properties that make them usable in applications where standard nonmagnetic fluids are the traditional solution.

This paper presents an experimental actuator that uses a magnetic nanofluid. It is divided in three sections. The first one presents the working magnetic nanofluid. The second section describes the electronic control of the actuator, and the third is devoted to mathematical modeling and numerical simulation of the magnetic field – magnetic fluid interaction. Fine details, such as local spectra of magnetic field, flow and heat transfer, and the magnetic fluid action to changes in the incident magnetic field may be discernable sometimes by numerical simulations only [2], [5], [7], [10], [11].

II. THE MAGNETIC NANOFLUID

The ferrofluid used in this application is a stable, colloidal suspension of sub-domain magnetic particles dispersed in a liquid carrier. The particles, of an average size of about 100 Å (10 nm), are coated with a stabilizing dispersing agent (surfactant), which prevents their agglomeration even when external magnetic field gradients act.

The surfactant must be matched to the carrier type and must overcome the van der Waals and magnetic attraction forces between the particles. In the absence of a magnetic field, the magnetic moments of the nanoparticles are randomly distributed hence the fluid has no net (macroscopic) magnetization [13], [14].

In an external magnetic field the magnetic moments of the nanoparticles in the nanofluid align up to the field lines almost instantly and they react immediately to the changes in the applied magnetic field. The forces holding the magnetic fluid in place are proportional to the gradient of the external field and the magnetization of the fluid.

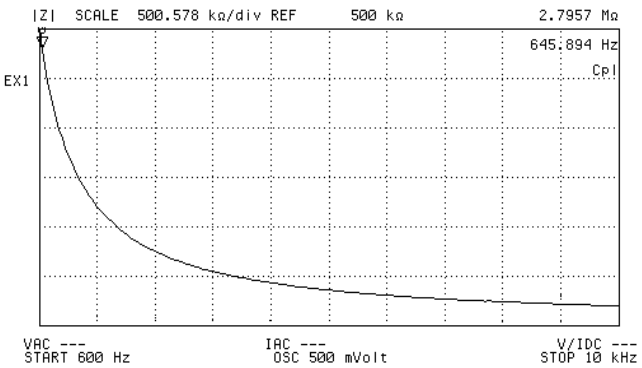

Fig. 1. Electrical impedance for 600 Hz…10 kHz.

The electrical impedance of the magnetic fluid was measured in the frequency range 600 Hz…10 kHz, of interest in this application. A significant decrease from 3 MΩ (at 600 Hz) to 0.5 MΩ (at 5 kHz) is noticeable. Above 5 kHz the impedance is relatively constant (Fig. 1).

The loss tangent variation was measured in the frequency range 0.60 Hz…1 kHz. It decreases from 1.3 (at 40 Hz) to 0.6 (at 700 Hz). Below this limit it has a relatively constant value, 0.55 (up to 1 kHz), Fig. 2.

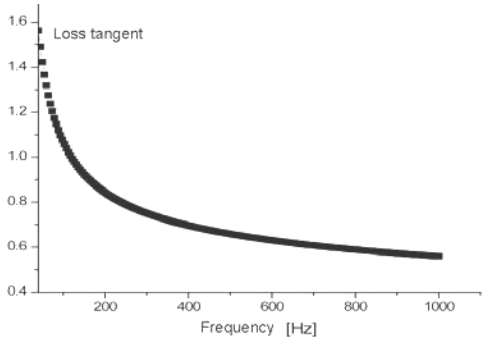

Fig. 2. Tangent of loss angle in the frequency range 0.60 Hz – 1 kHz

The measurements show that the magnetic nanofluid has good stability and adequate properties for the purpose of the experiment [15].

III. The Electronic Control

The experimental layout for testing the microactuator with magnetic fluid is shown in Fig. 3.

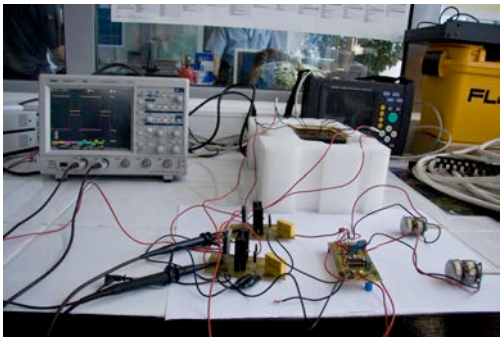

Fig. 3. Experimental layout used for testing the microactuator.

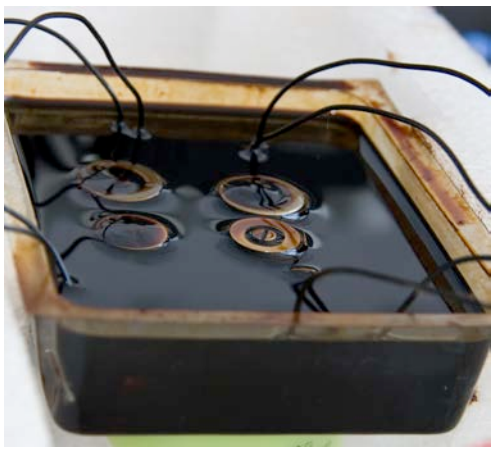

Fig. 4. Microactuator cell. All coils are powered. Although some fluid was removed to expose the coil, stationary waves are still noticeable.

The microactuator cell is presented in Fig. 4. A certain amount of fluid was removed to expose the four ferrite-cored coils. The waves produced by the magnetic field are still noticeable. The actuator is driven with rectangular pulses of constant frequency and of variable duration. Each pulse produces motion in the fluid, which is evidenced through stationary surface waves (Fig. 4).

The actuator electronic control that delivers the pulses implements the *pulse width modulation* (PWM) principle. A short duration pulse triggers a low current through the microactuator, and a long duration pulse triggers a higher current. The RMS value of the current passing through the actuator, for a fixed frequency of the PWM cue voltage, depends mainly on the pulse duty factor, *k*.

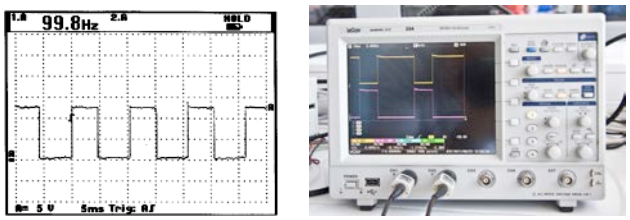

Fig. 5. The U_{out} waveform used to control the microactuator.

Fig. 5 shows the waveform of U_{out} for a pulse duty factor $k = 0.5$, and the frequency $f = 100$ Hz.

The block-diagram for the control of the frequency and duty cycle implemented with a DRV101T controller is depicted in Fig. 6, which shows the different continuous voltage sourcing modes of the final power stage for the controller and for the buffer.

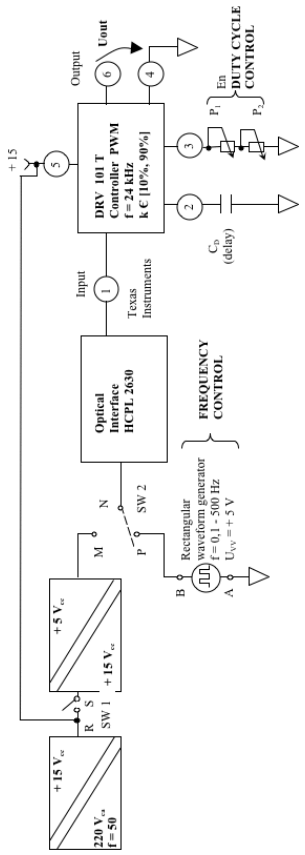

Fig. 6. Frequency and duty cycle module.

The final power stage is powered by an external continuous voltage source. The PWM controller and the auxiliary electronic circuits are powered by a 15 Vcc internal, stabilized continuous voltage source. The currents in the actuator coils depend on the ratio between the pulse duration and the PWM signal period.

The pulse duty factor may be adjusted as follows.

a) The potentiometers P1 (1 MΩ) and P2 (100 kΩ) are connected in series between pin 3 of the PWM wavelength controller and ground (Fig. 6). P1 provides for the gross adjustment of the pulse duty factor k while P2 provides for the fine-tuning. The pulse duty factor is adjustable within the range k = 10%...90%.

b) A rectangular pulse with the amplitude U_d = 5 V and of variable frequency f = 1…250 Hz, produced by an external generator, is applied on pin 1. The ferrofluid actuator enters an oscillatory mode resulting in a periodic motion of the nanofluid, with the same frequency.

An IGBT buffer (built of the complementary transistors BD 139 and BD 140 and ancillary components) is placed between the gate of the power IGBT (controlled by voltage pulses) and the pin 6.

IV. The Mathematical Model for the Magnetic Field, Fluid Flow, and Heat Transfer in the Microactuator

A subject of concern in the design of the microactuator is the interaction between the magnetic field and the magnetic fluid. The current carrying coils are submersed, covered by a shallow layer of magnetic fluid. The magnetic field produced by the actuator coils magnetizes the fluid and generates magnetic body forces that entrain the fluid. The fluid motion is perceived at the free surface through stationary waves that evidence the regions of higher gradients of magnetic field.

The mathematical model that describes the physical processes within the cell accounts for the magnetic field (Maxwell's equations), the magnetic fluid flow (momentum and mass conservation), and the heat transfer within the cell (energy equation). It is solved for numerically, by the finite element method (FEM). Simulation results, the messages they convey, and some useful design solutions that they suggest close this section.

A. The Magnetic Field

The magnetic field (induction currents) is periodic, described by the partial differential equation (PDE) for the magnetic vector potential [16]

$$\sigma\frac{\partial \mathbf{A}}{\partial t}+\nabla\times\left(\mu_0^{-1}\nabla\times\mathbf{A}-\mathbf{M}\right)=\mathbf{J}^e, \qquad (1)$$

where $\mathbf{A}$ [T·m] is the magnetic vector potential, $\mathbf{M}$ [A/m] is the magnetization (within the magnetic fluid), $\mu_f = \mu_0\mu_r$ [H/m] is the magnetic permeability, σ [S/m] is the electrical conductivity; $\mathbf{J}^e$ [A/m^2] is the external electric current density (in the coils windings).

The magnetic fluid magnetization is approximated by the analytic formula

$$M=\alpha\arctan(\beta H), \qquad (2)$$

where H [A/m] is the magnetic field strength, and α, β are dimensionless empiric constants selected to accurately model the magnetization of the magnetic fluid (Fig. 7). Here α = 3,050 A/m, and β = 1.5×10^{-5} m/A.

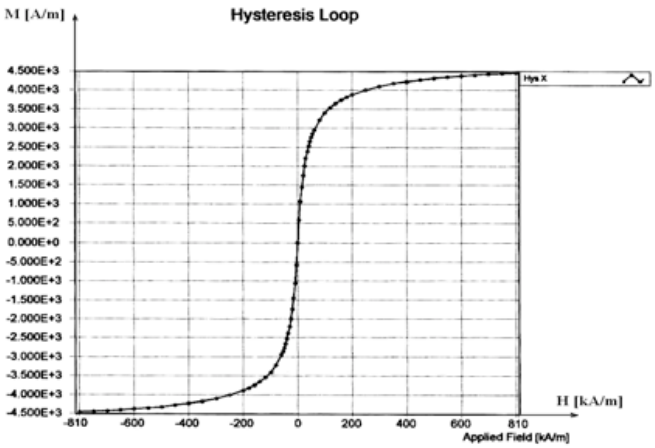

Fig. 7. The characteristic of magnetization for the magnetic fluid [15].

The magnetic fluid is super-paramagnetic hence when the magnetic field is suppressed the fluid becomes magnetically neutral. Conversely, in an external magnetic field body forces may occur, resulting in the fluid flow control [4], [11]. This behavior recommends the fluid as active medium for the actuator.

B. The Flow in the Magnetic Fluid

The forced flow produced by the magnetic body forces is described by the following PDEs [17]

Momentum balance (*Navier-Stokes*)

$$\rho\left[\frac{\partial \mathbf{u}}{\partial t}+(\mathbf{u}\cdot\nabla)\mathbf{u}\right]=-\nabla p+\underbrace{\mu_0(\mathbf{M}\cdot\nabla)\mathbf{H}}_{\mathbf{f}_{mg}}+\eta\nabla^2\mathbf{u}-\rho\mathbf{g}, \qquad (3)$$

Mass conservation (*incompressible flow*)

$$\nabla\cdot\mathbf{u}=0, \qquad (4)$$

where ρ [kg/m^3] is mass density, $\mathbf{u}$ [m/s] is the velocity, p [N/m^2] is the pressure field, $\mathbf{f}_{mg}$ [N/m^3] is the magnetic body force (within the ferrofluid), η [N·s/m^2] is the dynamic viscosity, $\mathbf{g}$ [m/s^2] is the gravity (acts vertically, in negative *Oz* axis direction).

The magnetic body forces are, formally, the derivatives of the magnetic energy with respect to the coordinates

$$\mathbf{f}_{mg}=\mu_0(\mathbf{M}\cdot\nabla)\mathbf{H}. \qquad (5)$$

Apparently, magnetic fields of higher degree of spatial uniformity do not produce significant body forces hence fluid entrainment. Thus it is expected that their effect is important in non-uniform magnetic fields. The simulation results are consistent with this observation.

The device generates heat, which is exhausted to the environment by temperature gradients that drive heat fluxes from the regions with heat sources throughout the system to the ambient. Thus, the magnetic fluid conveys the heat produced in the windings to the cell case and to the free surface of the pool, where it is further transferred to the environment. Within the fluid, heat is transferred

by convection. Within the other parts of the actuator, conduction is the heat transfer mechanism. The fluid is assumed opaque hence no internal radiation heat transfer occurs between the different parts of the device.

Energy equation

$$\rho c_p\left[\frac{\partial T}{\partial t}+\left(\mathbf{u}\cdot\nabla\right)T\right]=k\nabla^2 T+Q\,. \qquad (6)$$

Here, c_p [J/(kg·K)] is the specific heat, k [W/(m·K)] is the thermal conductivity, and Q [W/m^3] is the (Joule) heat source. The thermal properties of the model are linear.

Because, as it will be seen, the heat sources in the microactuator are less intense, heat transfer is a problem of less concern here. However, we decided to include it in the numerical simulations program.

The boundary conditions that close the model are:

- the magnetic fluid "confines" the magnetic field (the free surface and the containing case walls) and thus its surface acts as magnetic insulation;
- the device stands on an adiabatic support hence no heat transfer occurs through the cell bottom;
- all other parts of the case are cooled by moderate natural convection (h = 2 W/m^{2}K), and no heat transfer by radiation occurs;
- the case and the walls of the solid parts inside the cell are no-slip (zero velocity) boundaries;
- the upper surface is an open-boundary. Here a normal stress condition is assumed (**I** is the unity matrix, **n** is the normal to the surface, $(\cdot)^T$ is the transposition operator) [18]

$$\left[-p\mathbf{I}+\eta\left(\nabla\cdot\mathbf{u}+\left(\nabla\cdot\mathbf{u}\right)^T\right)\right]\cdot\mathbf{n}=0\,. \qquad (7)$$

On closing this section, a qualitative analysis of the problem is necessary to size the time scales that drive the couplings between the three different processes that act concurrently, and which may provide information useful in defining an optimal numerical solution strategy to the problem. Three time scales characterize the magnetic field-flow and heat transfer interactions: a (small, fast), magnetic time scale, $\tau_{0,mg}$, a (medium) flow time scale, τ_f, and a (slow, large) heat transfer time scale, τ_{ht}. These time scales add to the electric time scale provided by the electronics of actuation, τ_{eln}.

B.1 The magnetic time scale

The scaling relation associated to eq. (1) is

$$\frac{\sigma A_0}{t_{0,mg}},\frac{1}{L}\left(\frac{1}{\mu_0}\frac{A_0}{L},M_0\right)\sim J_0\,, \qquad (8)$$

where A_0, $t_{0,mg}$, M_0, L, J_0 are the scales of the vector potential, time, magnetization, length, and current density. Equation (1) may be rewritten as

$$\frac{\sigma\mu_0 L^2}{t_{0,mg}},\left(1,\mu_0 L\frac{M_0}{A_0}\right)\sim\mu_0 L^2\frac{J_0}{A_0}\,, \qquad (9)$$

which points out the magnetic time scale. Assuming that the "eigen" volume associated to an actuator (coil) has the length scale L = 0.02 m, and σ_{fluid} = 1 S/m yields $t_{0,mg}\sim O(10^{-5})$ s. Therefore the rise and fall times of the magnetic body forces is (technically) almost zero, and the dynamics of the magnetic fluid is governed by the mechanical time scales, explained next.

B.2 The flow time scale

The scaling relation associated to eq. (3) is

$$\rho\left[\frac{U_0}{t_0},U_0\frac{U_0}{L}\right]\sim\frac{P_0}{L},\mu_0 M_0\frac{U_0}{L},\eta\frac{U_0}{L^2},\rho g\,, \qquad (10)$$

where U_0, $t_{0,fl}$, P_0 are the scales for velocity, time, and pressure. This scaling relation may be rewritten as

$$\left(\frac{L}{U_0}\frac{1}{t_0},1\right)\sim\frac{P_0}{\rho U_0^2},\frac{\mu_0 M_0 H_0}{U_0^2},\frac{\nu}{U_0 L},\frac{gL}{U_0^2}\,, \qquad (11)$$

that yields the time scale

$$t_{0,fl}=L/U_0\,. \qquad (12)$$

The scale for magnetization, M_0, may be inferred by using Ampere's law, $\oint_\Gamma\mathbf{H}\cdot\mathbf{ds}=\Theta_{S_\Gamma}$, and eq. (2)

$$H_0 L_0/2\sim\Theta_{S_\Gamma},\quad M_0\sim\alpha\beta H_0. \qquad (13)$$

yielding $H_0\sim\Theta_{S_\Gamma}/\left(L_0/2\right)$ and $M_0\sim\alpha\beta\left[\Phi_{S_\Gamma}/\left(L_0/2\right)\right]$. Here Θ_{S_Γ} [A] is the total current in the coil (in this case, 400 A), and H_0 is the magnetic field strength scale.

The velocity scale is not readily available. There are two flow regimes that might have different velocity scales. They correspond to (a) the excitation, when the coil is powered (in this regime the magnetization body forces are acting – the second term in the right hand side of eq. (11)), and (b) the relaxation, when the current is switched off (the last term in the right hand side of eq. (11)). These quantities yield the following scales for velocity

$$U_0^{(mg)}=\sqrt{\frac{\mu_0 M_0 H_0}{\rho}}=\sqrt{\frac{\alpha\beta\mu_0}{\rho}}\frac{\Theta_{S_\Gamma}}{(L/2)}\,, \qquad (14,a)$$

$$U_0^{(g)}=\sqrt{gL}\,, \qquad (14,b)$$

which, when substituted in eq. (12), provide for the actuator under investigation $t_{0,fl}^{(mg)}\sim 0.02$ s and $t_{0,fl}^{(g)}\sim 0.045$ s, *i.e.* the same order of magnitude.

B.3 The heat transfer time scale

The scale analysis of eq. (6) yields $t_{0,ht}=\sqrt{(\rho c_p)/k_T}\,L$. Here ρ = 884 kg/m^3, c_p = 1990 J/(kg·K), k_T = 0.156 W/(m·K) hence the heat transfer time scale is $t_{0,ht}\sim$ 70 s – much larger that the other time scales.

These findings are used to qualitatively analyze the couplings in this "multiphysics" problem, and justify the numerical solution strategy presented next. Further more, this time scale(s) analysis is important to any control scheme implemented for this actuator.

V. NUMERICAL SIMULATION RESULTS

The motion within the fluid is characterized by small velocity. It is then reasonable to assume that the motion does not influence significantly the magnetic field and thus decouple it, and solve it first, independently.

The resulting body magnetic forces (by magnetization) and the resistive (active) power are input to the fluid flow problem (3)-(5) and (7), solved next. Finally, the heat transfer problem (6) is solved – in view of the weak coupling. The working regime of the actuator is periodic therefore dynamic (transient) simulation is used.

The mathematical model (1)-(7) is solved thorough Galerkin FEM, as implemented by Comsol Multiphysics [18]. The simulation time is extended until the quasi-steady state is reached. This was checked with respect to the specific force on the surfaces of the heads of the screws that fasten the coils (for 2D models) [15], and the magnetic flux density at the interface between the ferrite core and the magnetic fluid (the 3D model).

Because 3D models require significant hardware resources a simpler 2D model, where the computational domain is a "slice" cut through the full 3D model, was first considered (Fig. 8,a).

The results for the 2D model are reported elsewhere [15]. Here we present only the flow field and the deformation of the magnetic field free surface in response to the magnetic field produced by one of the coils of the actuator (Fig. 8,b) – the flow field by gray map and arrows for the velocity. The deformation is amplified *approx*. 31 times for better viewing.

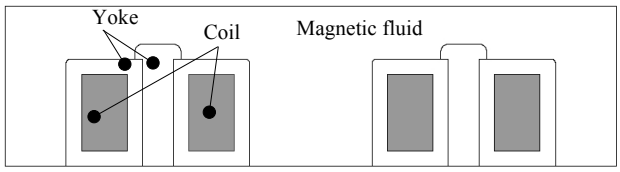

a. Computational domain – 2D model.

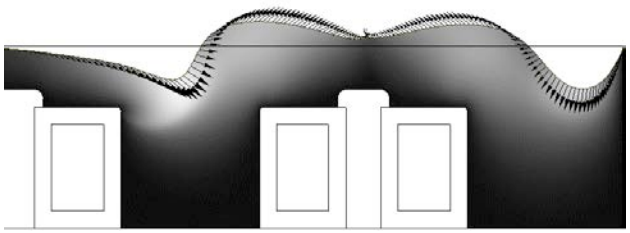

b. Flow field and the deformation of the free surface. The deformation is amplified for better viewing.

Fig. 8. The 2D model [15].

The morphology of the stationary waves in this 2D model should be compared with the findings in the 3D model, presented next. The numerical simulations are much more demanding in what concerns the software and hardware resources, therefore, symmetries are used to reduce the complexity of the computational models.

Fig. 9 shows the computational domain and the FEM mesh generated by Delaunay technique. Symmetry is used to reduce its size. Typically, meshes of roughly 13,000-14,000 tetrahedral, Lagrange quadratic elements led to converged, accurate solutions.

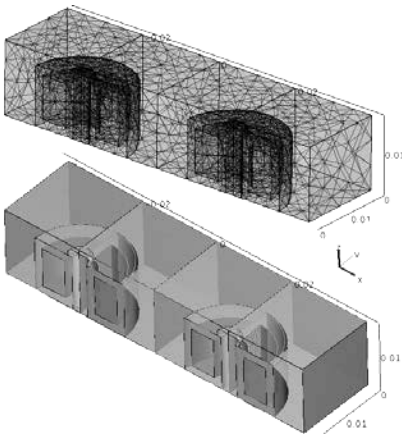

Fig. 9. The computational domain for the microactuator.

The magnetic field was solved first (periodic working conditions). It is the source for the (magnetization) body forces. Periodic working conditions were reached after 10-20 periods, for $f = 100$ Hz and $k = 0.5$.

The magnetic field is then solved again, this time together with the flow problem, using the previous (stored) magnetic field solution. The reason for this approach is of a technical nature, related to the calculation of the magnetic body forces. The main outcome of this phase is the deformation on the free surface of the magnetic fluid.

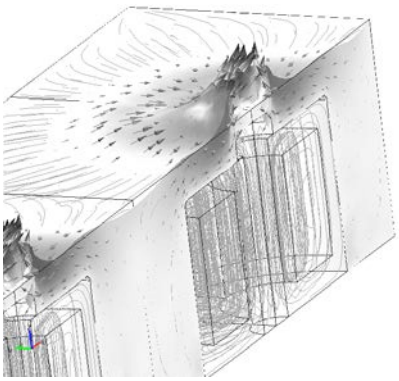

a. The wavy surface – gray map for deformation (proportional to the velocity field), arrows for the velocity field, and streamlines for the magnetic flux density.

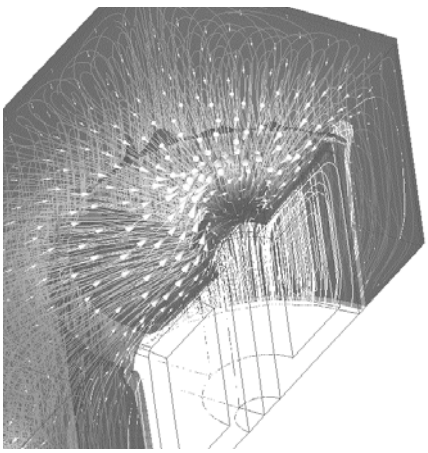

b. The flow and the magnetic field. The surface deformation (gray map) is proportional to the velocity field (arrows).

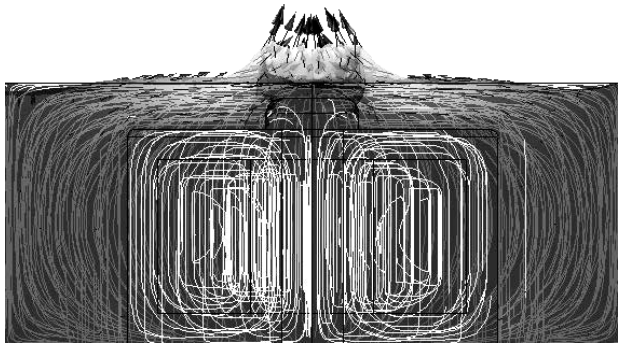

c. The flow and the magnetic field. The surface deformation (gray map) is proportional to the velocity field (arrows). Front view.

Fig. 10. Magnetic field, magnetic fluid flow, and deformation by numerical simulation, at t = 2.1 s, when the two coils are switched.

This solution strategy was implemented numerically by using the UMFPACK iterative solver [18] that provides for a multithread approach to solve the algebraic system of equations. Fig. 12 shows details of the simulation results of the flow field. Deformations are amplified for better viewing. The resistive (active) power in the windings is the heat source (Joule) in the heat transfer problem, which is solved for, finally.

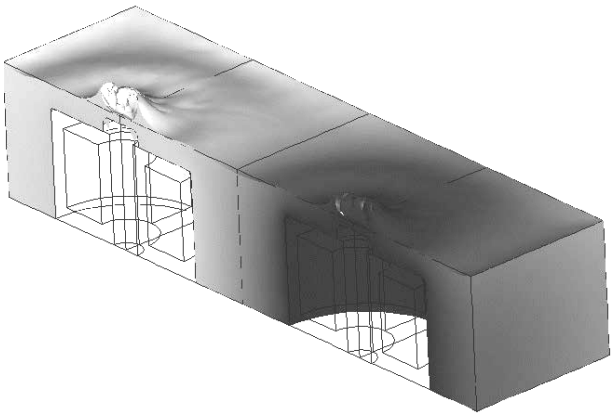

a. The temperature distribution related to the wavy free surface.

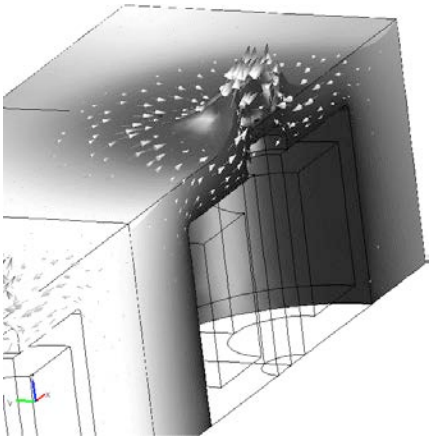

b. Detailed view of (c). The surface velocity is also shown.

Fig. 11. Heat transfer simulation results at t = 2.1 s, when the two coils are switched.

Fig. 13 displays isotherms and slices of gray maps for the temperature field. In all cases the amperturns are balanced, and the working conditions are nominal. The heat source is clearly seen in the current active region.

The magnetic fluid is entrained in a convection motion that conveys the heat from the source to the free surface and the case walls, to be later exhausted to the ambient by natural convection, except for the bottom wall, which is assumed adiabatic.

The temperature of the device reaches 2-3 degrees above the ambient temperature hence the thermal stability of the actuator should be of no concern.

VI. CONCLUSIONS

This paper presents an experimental microactuator that utilizes a magnetic nanofluid. The core, specific part of the device is the super-paramagnetic fluid, which has adequate magnetic properties to provide for a fast reaction to external magnetic fields produced by electrical currents triggered by train pulses.

A dedicated electronic module, which implements the PWM principle, was designed to provide the train pulses of adjustable frequency and fill factor that are needed to control the electrical currents in a set a ferrite cored coils.

The magnetic field produced by these currents generates magnetic body forces within the magnetic fluid, resulting in the fluid entrainment in a forced flow. The magnetic forces are significant in the regions of higher magnetic field non-uniformity.

During the "on" interval of the duty cycle (the excitation phase) the fluid is driven by magnetic and gravitational body force. During the "off" interval (the relaxation phase) the gravitational forces drive the fluid to its rest state. The motion is observed through periodic stationary surface waves above the actuator coils.

A time scale analysis was conducted to assess the time scales of this magnetic fluid actuator. The results are used to analyze the couplings in this "multiphysics" problem, and to device the numerical solution strategy. Further more, this time scale(s) analysis is important to any control scheme implemented for this actuator.

The usage of a magnetic fluid implies the knowledge of the magnetization body forces that add to gravitational forces. Mathematical modeling and numerical simulation of the interaction magnetic field – magnetic fluid provides for valuable information on the processes that occur within the actuator cell. 2D and 3D analyses provide for fine details, such as local spectra of magnetic field, flow and heat transfer, and the magnetic fluid action to changes in the incident magnetic field that are discernable by numerical simulations only.

The overtemperature of the device is very small, so thermal stress should not be an issue.

Future research will be devoted to optimize the microactuator design – *e.g.*, adapt the fill factor and the duty cycle to the magnetic fluid properties – and to adjust its characteristics for specific applications.

ACKNOWLEDGMENTS

The numerical simulations were conducted in the Laboratory for Multiphysics Modeling, at UPB-EE. The design, prototyping and experiments on the magnetic fluid, the electronic control, and the microactuator cell were conducted at ICPE-CA.

REFERENCES

[1] FEROTEC Corporation Singapore, www.ferrotec.com, 2009.

[2] C. Tangthieng, B.A. Finlayson, J.S. Maulbetsch, T. Cader, "Heat Transfer Enhancement in Ferrofluids subjected to Steady Magnetic Field," *Eighth International Conference on Magnetic Fluids*, Timisoara, June 29-July 3, 1998.

[3] B. Berkovski, V. Bashtovoy (Eds.), *Magnetic Fluids and Applications,* Handbook, Begell House, New York, 1996.

[4] A.M. Morega, M. Morega, "A FEM analysis of magnetic induced biomagnetic fluid mixing," *Rev. Roumaine Sci. Techn. Electrotech. et Energ.*, **50**, 2, pp. 239-248, 2005.

[5] C. Tangthieng, B.A. Finlayson, J. Maulbetsch, T. Cader, "Heat transfer enhancement in ferrofluids subjected to steady magnetic fields," *J. of Magnetism and Magnetic Mat.* **201**, pp. 252-255, 1999.

[6] P. Filar, E. Fornalik, T. Tagawa, H. Ozoe, J. Szmyd, "Numerical and experimental analyses of magnetic convection of paramagnetic fluid in a cylinder," *J. Heat Transfer*, **128**, pp. 183–91, 2006.

[7] S.M. Snyder, T. Cader, B.A. Finlayson, "Finite element model of magnetoconvection of a ferrofluid," *J. of Magnetism and Magnetic Mat.* **262**, pp. 269-279, 2003.

[8] F. Schneider, D. Hohlfeld, U. Wallrabe, "Miniaturized electromagnetic ferrofluid actuator", ACTUATOR 2006, 10th Intl. Conference on New Actuators, 14–16 June 2006, Bremen, Germany.

[9] D.Brousseau1, E.F. Borra1, S. Thibault, "Wavefront correction with a 37-actuator ferrofluid deformable mirror", Astrophys. J. **393**, pp. 829-847, 1992.

[10] A.M. Morega, M. Morega, F.D. Stoian, S. Holotescu, "Numerical simulation of an experimental apparatus for the evaluation of physical properties of magnetic fluids", *COMSOL Conference*, Budapest, 24-25 November, 2008.

[11] L. Pîslaru–Dănescu, A.M. Morega, F. Nouraş, V. Stoica, "Thermal effects on functional characteristics of the electrical transformers," *ELECTROMOTION*, 2009.

[12] D. Bica, "Preparation of magnetic fluids for various applications," *Rom. Repts. Phys.*, **47**, (3-5), pp. 265-272, 1995.

[13] M. Raşa, "Magnetic properties and magneto-birefringence of magnetic fluids," *Eur. Phys. J. E*, **2**, 265-275, 2000.

[14] M. Raşa, D. Bica, A. Philipse, L. Vekas, "Dilution series approach for investigation of microstructural properties and particle interactions in high-quality magnetic fluids," *Eur. Phys. J. E*, **7**, pp. 209-220, 2002.

[15] L. Pislaru-Danescu, A.M. Morega, G. Telipan, V. Stoica, "Nanoparticles of ferrofluid Fe3O4 synthesized by coprecipitation method used in microactuation process", Optoelectronics and Advanced Materials – Rapid Communications **4**, 8, 2010, pp. 1182–1186, 2010.

[16] C.I. Mocanu, *Teoria câmpului electromagnetic*, Ed. Didactică şi Pedagogică, Bucureşti, 1981.

[17] A. Bejan, *Convection heat transfer*, Wiley, NY, 1984.

[18] COMSOL Multiphysics *User's Guide*, Version 3.5a, COMSOL A.B. Sewden, 2010.